Journal of
Microscopy

Journal of Microscopy, Vol. 00, Issue 00 2014, pp. 1–8 doi: 10.1111/jmi.12124
Received 5 September 2013; accepted 15 February 2014

Specimen-thickness effects on transmission Kikuchi patterns in the scanning electron microscope*

K.P. RICE*, R.R. KELLER* & M.P. STOYKOVICH†
Applied Chemicals and Materials Division, National Institute of Standards and Technology, Boulder, Colorado, U.S.A.
†*Department of Chemical and Biological Engineering, University of Colorado, Boulder, Colorado, U.S.A.*

Key words. Monte Carlo simulations, scanning electron microscopy, transmission EBSD, transmission kikuchi diffraction, ultrathin films.

Summary

We report the effects of varying specimen thickness on the generation of transmission Kikuchi patterns in the scanning electron microscope. Diffraction patterns sufficient for automated indexing were observed from films spanning nearly three orders of magnitude in thickness in several materials, from 5 nm of hafnium dioxide to 3 μm of aluminum, corresponding to a mass-thickness range of ~5 to 810 μg cm^{-2}. The scattering events that are most likely to be detected in transmission are shown to be very near the exit surface of the films. The energies, spatial distribution and trajectories of the electrons that are transmitted through the film and are collected by the detector are predicted using Monte Carlo simulations.

Introduction

The crystallographic structure and orientation of materials significantly affect their thermal (Jagannadham, 2011; Roh *et al.*, 2011), electrical (Jagar *et al.*, 2001), magnetic (Kleibert *et al.*, 2011), and mechanical properties (Vinci & Vlassak, 1996; Hu & Pan, 2009). Characterizing the degree of crystallinity and crystal orientation, size and texture is therefore crucially important to the reliability and performance of such materials, as well as any devices made thereof. In thin films, in particular, even small variations in microstructural defects, orientation and crystal phase become critical to the operation of a device (Jagar *et al.*, 2001; Lanza *et al.*, 2012), and often such crystallographic character is influenced by confinement of the material to small volumes, the processing conditions and the presence of interfaces (*e.g.* in epitaxial growth).

The scanning electron microscope (SEM) method of electron backscatter diffraction (EBSD) is used to rapidly characterize crystallographic structure over large surface areas of materials. The method takes advantage of Kikuchi scattering undergone by backscattered electrons. The EBSD technique has been applied to metals (Humphreys, 1999), geological samples (Prior *et al.*, 1999) and patterned thin films (Vanasupa *et al.*, 1999). Tilting the sample 70° towards the phosphor screen of the EBSD detector improves the signal obtained from the backscattered electrons, but spreads the beam across the sample and decreases spatial resolution perpendicular to the tilt axis. In the analysis of bulk material surfaces, this usually results in a lateral spatial resolution of better than 100 nm. The best reported resolution of the technique is ~20 nm (parallel to the tilt axis) by 60 nm (perpendicular to the tilt axis) during orientation mapping (Maitland & Sitzman, 2007); the factor of three difference is due to the effect of the high tilt angle on scattering normal to the tilt axis.

Recently, a new method of electron diffraction in the SEM has been reported, which was first denoted 'transmission EBSD' (Keller & Geiss, 2012) because of its use of conventional EBSD equipment. This technique, also known as transmission Kikuchi diffraction in the SEM (Trimby, 2012) or transmission electron forward scatter diffraction (Brodusch *et al.*, 2013a), is a modification of existing EBSD methods in which the beam passes through the sample, rather than reflecting off the surface of the tilted sample. Tilting a sample 10°–20° away from the EBSD camera allows electrons that transmit through the sample and undergo Kikuchi diffraction to be collected by the phosphor screen, creating patterns that appear similar to those in EBSD. The transmission EBSD technique is compatible with diverse material systems and sample geometries, and has been used to characterize metal and metal oxide nanoparticles (Geiss *et al.*, 2010; Brodusch *et al.*, 2013a), light-metal alloys (Brodusch *et al.*, 2013b) and to collect strain maps in thin Ni films (Trimby, 2012).

Eliminating the highly tilted sample geometry and collecting transmitted electrons provides advantages compared to

*Contribution of the National Institute of Standards and Technology, not subject to copyright.

Correspondence to: Katherine Rice, Applied Chemicals and Materials Division, National Institute of Standards and Technology, Boulder, CO 80305, U.S.A. Tel: 303-497-7996; Fax: (303) 497-5030; e-mail: katherine.rice@nist.gov

Published 2014. This article is a U.S. Government work and is in the public domain in the USA

analysing the backscattered electrons, particularly for small sample volumes, such as those associated with ultrathin films and nanostructures. A significantly higher percentage of the incident beam electrons are forward scattered, thus a pattern can be generated from smaller sampling volumes (and consequently less material) than required when using backscattered electrons. For example, clear, indexable patterns were obtained from sub-10 nm crystalline particles of Fe–Co (Keller & Geiss, 2012), representing an improvement of an order of magnitude over previous attempts to use reflection EBSD to analyse isolated particles (Small *et al.*, 2002). Resolution is also improved during crystallographic orientation mapping of thinned bulk materials, with effective mapping resolutions of 2–3 nm (Trimby, 2012, Brodusch *et al.*, 2013a) and 5 nm (Brodusch *et al.*, 2013a) having been reported.

Here we present the capabilities and limitations of transmission Kikuchi diffraction in the SEM for characterizing crystallographic structure in both thin and thick films, including ultrathin samples of interest to the semiconductor industry, micrometre-thick foil samples and bilayer film systems. Low-energy Kikuchi scattering results are discussed in the context of electron penetration and transmitted energy distributions as predicted using Monte Carlo simulations of electron trajectories within the material.

Experimental

Transmission Kikuchi diffraction in the SEM

An infrared image of the sample-detector configuration in the SEM is shown in Figure 1. The position of the sample grid is highlighted with a yellow line and the blue area indicates the EBSD detector. Samples were mounted on a commercially available SEM stub and the stage was tilted ∼15° from horizontal, with the sample normal tilted away from the EBSD detector. The field emission SEM used in this work was operated between 20 and 30 kV, in most cases with a 60 μm aperture, resulting in a probe current of ∼300 pA.

Materials and specimen preparation

Hafnium dioxide (HfO_2) films deposited by atomic layer deposition were annealed at 500°C for 180 s under N_2 to promote grain growth (Niinistö *et al.*, 2010). Two bilayer Au/Si_3N_4 samples were fabricated by depositing 10 nm of Au by thermal evaporation on commercially available amorphous Si_3N_4 substrates. Commercially available rolled aluminum foils were mounted in folding transmission electron microscopy (TEM) grids. All other samples were deposited on commercially available lacy carbon grids.

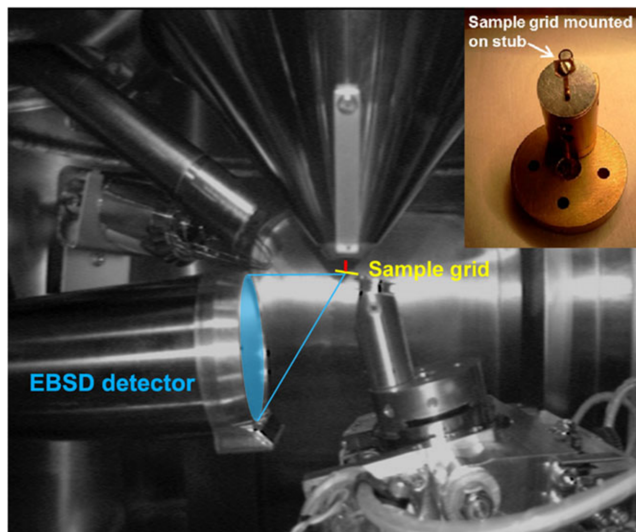

Fig. 1. Infrared image of the sample-detector configuration in the SEM. The sample grid is indicated in yellow and the range of potential scattering directions captured by the EBSD detector is highlighted in blue.

Monte Carlo simulations of electron trajectories

Electron trajectories through the thin films were calculated using an in-house Monte Carlo simulator that was programmed in Matlab,[1] and that implemented conventional models for electron scattering and energy loss (Joy & Luo, 1989; Joy, 1991). Discrete elastic and inelastic scattering events were considered, with the scattering cross-sections of the material specifying the probability of each type of scattering and the distance between scattering sites.

Results and discussion

Kikuchi scattering in films

Within films, the region from which transmission Kikuchi diffraction patterns are detected was determined by comparing two bilayer films of crystalline Au on amorphous Si_3N_4 (a-Si_3N_4). Specimen 1 consisted of a 10 nm layer of polycrystalline Au on a 20 nm a-Si_3N_4 layer, whereas Specimen 2 consisted of 10 nm polycrystalline Au on a 50 nm a-Si_3N_4 layer. Each specimen was characterized by transmission Kikuchi diffraction in two orientations relative to the incident electron beam and the detector. Figure 2 shows images of the EBSD phosphor collected with the specimens oriented such that the Au film was 'facing up', *i.e.* the incident beam impinged on the gold film and the diffracted beams exited from the nitride film. Diffuse, but recognizable, patterns (Fig. 2A) were observed for

[1] Certain commercial equipment, instruments or materials are identified in this paper in order to specify the experimental procedure adequately. Such identification does not imply recommendation or endorsement by National Institute of Standards and Technology, nor does it imply that the materials or equipment identified are necessarily the best available for the purpose.

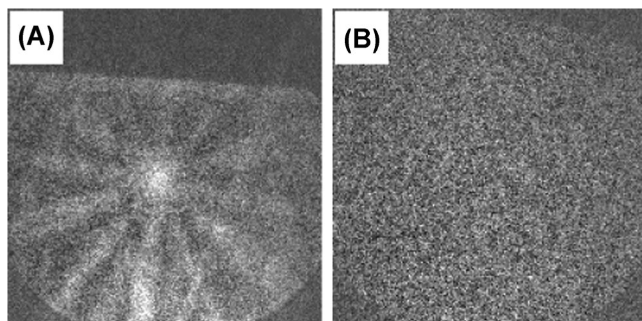

Fig. 2. EBSD phosphor images from bilayer films with electrons incident on polycrystalline gold: (A) 10 nm Au/20 nm amorphous Si_3N_4 and (B) 10 nm Au/amorphous 50 nm Si_3N_4.

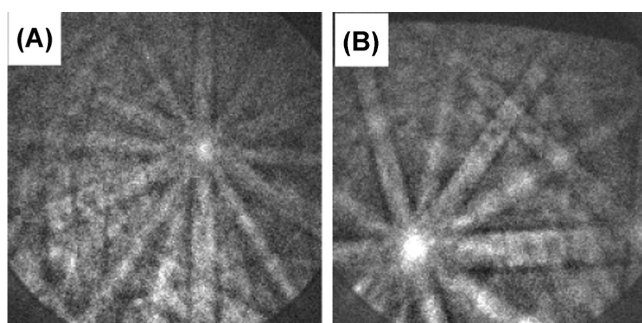

Fig. 3. EBSD phosphor images from bilayer films with electron incident on amorphous silicon nitride (A) 10 nm Au/20 nm Si_3N_4 and (B) 10 nm Au/50 nm Si_3N_4.

the 10 nm poly-Au/20 nm a-Si_3N_4 bilayer. Conversely, no patterns could be obtained for the 10 nm poly-Au/50 nm a-Si_3N_4 bilayer.

Figure 3 shows images of the EBSD phosphor collected with the specimens oriented such that the Au film was 'facing down', *i.e.* the incident beam impinged on the nitride film and the diffracted beam exited from the gold film. Patterns are readily seen for both specimens with the thinner and thicker nitride layers. A qualitative comparison with Figure 2 reveals that the Kikuchi patterns obtained in the Au facing down orientation show more contrast and greater pattern sharpness.

From these bilayer experiments, it can be concluded that the scattering events of prime importance to the formation of a transmission Kikuchi diffraction pattern occur near the exit surface of the specimen. If Kikuchi scattered electrons traverse little to no material before exiting the specimen, then high contrast Kikuchi patterns should be observed. Even a thin layer of amorphous material beneath the crystalline material of interest, *e.g.* 50 nm of a relatively electron transparent material such as Si_3N_4 as shown here, can cause Kikuchi scattered electrons from the crystalline layer to undergo additional scattering events and a loss of the diffraction pattern.

The importance of near-exit surface Kikuchi sources in transmission is consistent with observations during conventional backscattered EBSD that the important Kikuchi scattering events originate only within the top few tens of nanometres of a crystalline film (Dingley, 2004), with the scattering volume dependent on atomic number. For Kikuchi scattering events occurring deeper in the film, the diffracted electrons will continue to scatter until they return to the near-exit surface region and will not contribute to the Kikuchi pattern (and will instead contribute to the background signal) unless they undergo additional Kikuchi scattering. In comparison to SEM techniques for electron diffraction, determining the location of detectable Kikuchi diffraction is generally not a concern in TEM techniques. Electrons at order-of-magnitude higher TEM energies are significantly less likely to scatter in nanoscale specimens, due to smaller scattering cross-sections and longer mean free paths, and thus sampling volumes for Kikuchi diffraction are much larger and the probabilities associated with post-diffraction scattering events are low.

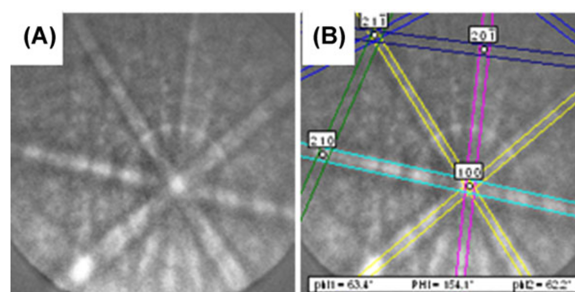

Fig. 4. Kikuchi diffraction pattern from a 5 nm HfO_2 film: (A) raw data and (B) with indexing overlaid showing the monoclinic crystal phase of HfO_2.

Kikuchi diffraction from ultrathin films

The relatively shorter scattering path lengths for electrons in transmission Kikuchi diffraction in the SEM suggests that the technique may be well suited to the characterization of ultrathin films. One such ultrathin film is HfO_2, used as a gate dielectric in state-of-the-art transistors. Performance of the HfO_2 gate dielectic layer is highly dependent on crystallographic properties such as phase, grain size and orientation (Chen *et al.*, 2008), and a technique that could reveal local spatial variations in these properties would be valuable. Here we assess whether Kikuchi diffraction in transmission can be used to determine crystallographic phase in HfO_2 films of thickness 5 nm. The film was formed by atomic layer deposition onto carbon-coated TEM grids, and thermally annealed to induce crystalline grain growth. The specimens were positioned in planview, and the SEM was operated at an accelerating voltage of 20 kV.

Figure 4(A) shows a Kikuchi pattern obtained from the 5 nm HfO_2 film, and Figure 4(B) shows pattern indexing to the $P2_1/c$

monoclinic space group with commercially available software. Deal *et al.* (2008) suggested that a fundamental lower limit in specimen thickness for Kikuchi scattering associated with EBSD (as well as TEM-based Kikuchi diffraction) is approached at approximately one-fourth of an electron extinction distance. Thinner specimens result in thickness-dependent broadening of the Kikuchi bands, which leads to blurring and a loss of contrast in the pattern. In monoclinic HfO_2, for a low-index reflection such as 0 1 1, the associated extinction distance for 20 keV electrons is ~27 nm, a quarter of which is ~7 nm. The pattern in Figure 4 qualitatively exhibits some blurring, perhaps consistent with the suggestion that a lower limit in film thickness is being approached under these conditions. However, pattern indexing remains reliable as long as the diffraction patterns have sufficient contrast. An advantage of transmission Kikuchi diffraction in the SEM is that the yield of forward-scattered electrons is high, even with lower-energy electrons that have shorter extinction distances and that may allow interrogation of films even thinner than 5 nm.

Kikuchi diffraction from thick films

The relatively low energies of SEM electrons initially seem like they may present a disadvantage for obtaining diffraction patterns in transmission for thicker films. For example, in conventional TEM imaging (*e.g.* bright-field, two-beam conditions) of low- to mid-range atomic number metals such as Al or Cu at relatively low magnifications (*e.g.* <50 k magnifications), one typically seeks specimens with thicknesses in the approximate range 150–200 nm for imaging with 120–200 keV electrons. Significantly thicker specimens tend to yield images that show little contrast or are too dark for quantitative analysis of features such as defect or grain structure. However, such specimen limits are not determined by the ability of the electron beam to penetrate that much material.

In conventional EBSD, thicker films are not typically a problem, since in this surface sensitive technique the Kikuchi pattern is formed by electrons that have penetrated less than approximately 40 nm into the film (Dingley, 2004). Pattern contrast in reflection primarily comes from 'low-loss' backscattered electrons, or those that have retained greater than 90% of the incident beam energy ($E_{incident}$), in which the near-surface high-energy electrons are the primary contributors to the pattern (Deal *et al.*, 2008). In the transmission arrangement, energy losses due to scattering occur throughout the entire film thickness prior to the detectable Kikuchi scattering events near the exit surface. This energy loss may be significant for thick films, and there exists an upper thickness limit beyond which no electrons are transmitted. It is therefore necessary to establish a new reference in transmission for what is considered 'low-loss' when referring to electrons that Kikuchi diffract out of the bottom surface of the specimen.

Monte Carlo simulations of electron scattering in materials can provide estimates of energy losses in thicker films, and thus the energies of the electrons that are contributing to Kikuchi pattern contrast. Figure 5(A) shows the energy losses and transmitted electron yields through the film as simulated by Monte Carlo for the thickest aluminum films that were investigated. Each data point is the result of 10 simulations of 1000 electrons with a 30 keV incident energy ($E_{incident}$). Standard models for electron scattering and energy loss were used in the code, written in-house and programmed in Matlab (see footnote 1). The graph shows the percentage of the incident electrons that were transmitted for three cases: (1) the total transmitted electrons, regardless of their energy at the exit surface (blue circles), (2) electrons that retained $\geq 90\%$ of the incident beam energy (red circles) and (3) electrons that retained $\geq 90\%$ of the maximum transmitted energy for that film thickness (black triangles). The maximum transmitted energy, or E_{max}, was determined for an idealized straight path through the film, a schematic of which can be seen in Figure 5B(top). The magnitude of E_{max} was determined using a continuous slowing down approximation based on Bethe's stopping power equation for electrons, and estimates the energy losses if an electron does not undergo discrete scattering events that would cause it to change directions and therefore take a longer path in the film.

The inset images in Figure 5 show Kikuchi patterns obtained for Al films at 1500, 2000 and 3000 nm in thickness. None of the conventional low-loss electrons ($\geq 90\%$ of $E_{incident}$) are predicted to reach the exit surface for the thickest Al films, yet it is clear that indexable Kikuchi patterns can nonetheless be acquired. E_{max} for electrons that were transmitted through 1500 and 3000 nm of Al are 26.4 and 22.3 keV, respectively. A marked decrease in pattern quality and contrast is observed in the thicker Al films, which is thought to result from the coupled effect of a lower detected signal due to fewer electrons being transmitted and electron energy losses due to multiple scattering events, especially post-Kikuchi scattering. Approximately 20% of the electrons incident to 3000 nm Al films are transmitted and have energies greater than 90% of E_{max}, which is proposed here to be a more appropriate reference for Kikuchi pattern generation in transmission. Although electrons of any energy can contribute to a Kikuchi pattern, it is the highest-energy transmitted electrons that have been scattered the least and taken the most direct path through the film. These electrons more probably contribute to the diffraction pattern because they are less likely to have experienced changes in trajectory or energy after Kikuchi scattering and do not contribute significantly to beam broadening.

Energy distributions and trajectories for electrons transmitted through thick Al films are shown in Figure 6 as predicted by the scattering simulations. The panels on the left consider all of the electrons transmitted through the film, while the panels on the right consider only those electrons that reach the detector as specified by the geometry in Figure 1 (the sample tilted 15° from the incident beam, and the detector encompassing 70° in the latitudinal and longitudinal directions

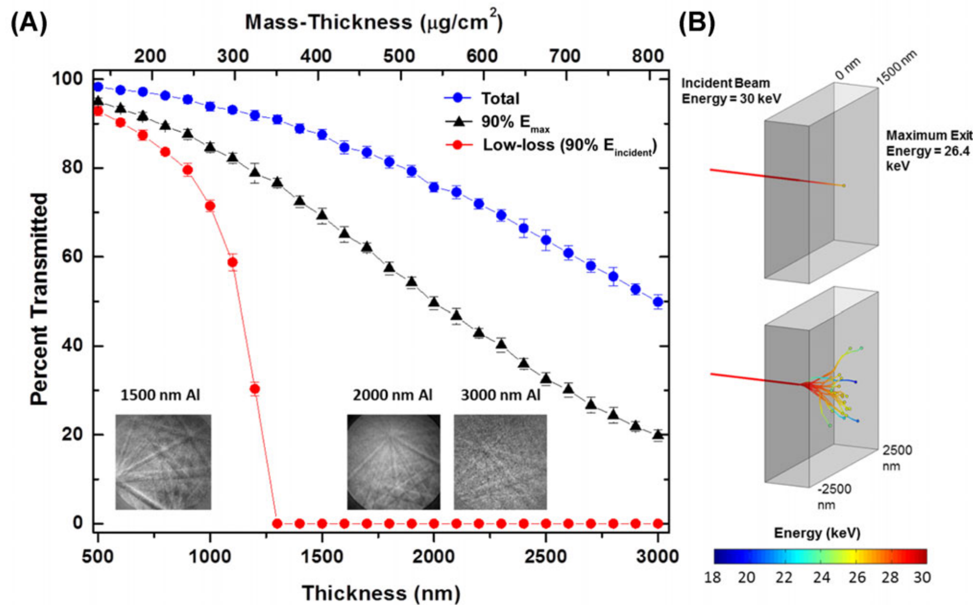

Fig. 5. (A) Electron scattering simulation results for the fraction of incident electrons that transmit through Al films as a function of specimen thickness (bottom axis) and mass-thickness (top axis). Blue data represent total electron transmission. Black data represent transmission of electrons that retain at least 90% of the maximum possible energy at the exit surface (see text for details). Red data represent transmission of electrons that retain at least 90% of the incident beam energy. Insets show Kikuchi diffraction patterns obtained from Al films at the indicated thicknesses, at an incident beam energy of 30 keV.(B) Top: Schematic of shortest possible electron path through a 1500 nm film of Al. These electrons have not undergone changes in trajectory, but were subject to energy losses approximated by a modified Bethe stopping power equation. This idealized path is associated with maximum energy retention at the exit surface, 26.4 keV in this case. Bottom: Schematic of trajectories of 25 electrons that have undergone both elastic and inelastic scattering in the usual manner within a 1500 nm film of Al. Trajectories are colorized based on their local energy in space. The incident electrons had an incident energy of 30 keV.

from 15° to 85° from the sample normal). The colours of the trajectories indicate the electron energy at the exit surface, and it is assumed that they undergo a straight path through vacuum to the detector after exiting the film. The top insets show a three-dimensional side view profile of the electron paths after being transmitted through the sample (yellow puck), and the bottom insets indicate a top-down view with the position of the detector shaded in blue for the distributions at right.

Considerable broadening of the energy distributions occurs with increases in the film thickness, which undoubtedly contributes to lower contrast in the Kikuchi diffraction patterns in thicker films. Integration of the energy distribution curves indicates the proportions of electrons that transmit and those that strike the EBSD detector, with results shown in Table 1.

The low yield to the detector position in the 500 nm Al film is the result of the relative prominence of low-angle forward scattering events, in contrast to high-angle forward or backward scattering events, such that the majority of transmitted electrons do not scatter to angles large enough to reach the detector (inset, Fig. 6A). Surprisingly, a higher percentage of the electrons that make it through the film actually reach the detector in the thicker films, in this case because the electrons are more likely to undergo multiple scattering events and to scatter to the wide exit angles necessary to reach the detector as positioned in Fig 1. The Monte Carlo simulations also indicate that the energies of the transmitted electrons and those that reach the detector are the same, *i.e.* the electron energy distributions in Figure 6 at a given film thickness are nearly identical if normalized to the total area, so the position of the phosphor screen does not affect the sampling.

Although Kikuchi patterns can be acquired from very thick samples, the effects of beam broadening due to electron scattering become stronger in increasingly thick specimens and lead to degradation of the lateral spatial resolution. The films in this work contained grains of diameter in the tens of microns, much greater than the film thickness; hence diffraction from multiple grains due to lateral beam spreading did not pose significant problems in the collection of isolated patterns. However, we point out that orientation mapping from such thick specimens would result in spatial resolutions considerably poorer than those seen by Trimby and Brodusch with thinner films (Trimby, 2012; Brodusch *et al.*, 2013a). We have found that the mass-thickness $x = \rho \times t$, where ρ is the density and t is the film thickness, may provide an appropriate heuristic for the range of film systems that can provide indexable patterns with transmission EBSD. Indexable patterns were obtained over a wide range of specimen mass thicknesses, from $\sim 5\ \mu g\ cm^{-2}$ (in 5 nm of HfO_2) to $\sim 810\ \mu g\ cm^{-2}$ (in 3 μm of

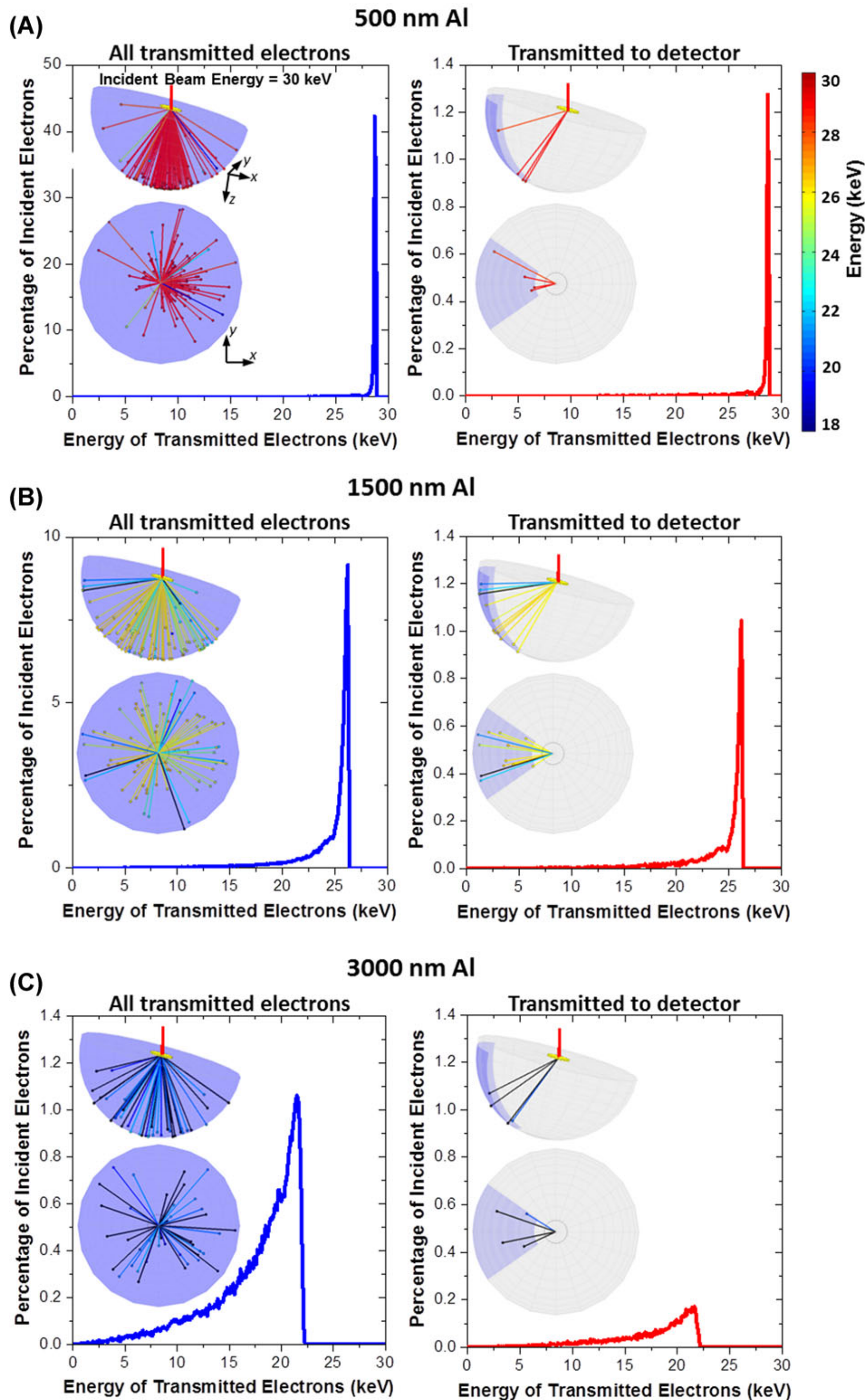

Fig. 6. Path of flight simulations of electrons transmitted through (A) 500 nm, (B) 1500 nm and (C) 3000 nm Al films to the surroundings. The electron paths on the left are shown for all transmitted electrons, whereas the paths on the right are only those that reach the detector and contribute to the EBSD signal. The detector is specified to be positioned at the blue surface, as estimated from measurements to be 24.1 mm from the sample and to encompass 70° in the latitudinal and longitudinal directions (see Fig. 1). The sample position is indicated by a yellow puck that is ~3 mm in diameter. The electron paths are shown for MC scattering simulations of 100 electrons with 30 keV energy incident to the sample at 15° from normal, as in the real experimental setup. Distributions of the energies of the transmitted (left, blue) and detected (right, red) electrons as calculated by the MC scattering simulations are also shown for each system and were simulated using 100 000 electrons each.

Table 1. Proportions of electrons transmitted through the film and to the detector position.

Film	Proportion of incident electrons transmitted	Proportion of incident electrons striking detector	Proportion of transmitted electrons striking detector
500 nm Al	98.0%	3.4%	3.4%
1500 nm Al	85.7%	9.2%	10.7%
3000 nm Al	47.4%	7.8%	16.4%

Al). Included in this analysis of effective working range were HfO_2 coatings, Al foils and evaporated Cu, Au and Ag thin films.

Conclusions

SEM-based transmission Kikuchi diffraction patterns can be obtained from specimens over a wide range of thicknesses, from 5 nm of HfO_2 (mass-thickness $\sim 5\ \mu g\ cm^{-2}$) to 3 μm of Al (mass-thickness $\sim 800\ \mu g\ cm^{-2}$) as shown in this study. Bilayer experiments demonstrated that pattern sharpness and contrast were strong when there is significant Kikuchi diffraction occurring very near the exit surface of the specimen. In the case of very thick specimens, this can come at the cost of nonnegligible lateral beam broadening; and this must be considered when making estimates of spatial resolution during orientation mapping. Monte Carlo calculations of electron scattering associated with the specimen-EBSD detector geometry suggested that diffraction patterns form with less than 10% of the incident electrons reaching the detector. For all but the very thickest of specimens, those electrons retain a relatively narrow energy distribution similar to that of the overall transmitted electron signal. Despite both the seemingly low signal and the shift of the distribution to lower energies due to increased scattering in thicker specimens, strong contrast may still be obtained in SEM-based transmission Kikuchi diffraction. We propose a new reference to low-loss electrons for transmission EBSD, with 90% of the maximum exit energy as an alternative threshold for electrons that may provide the strongest contrast.

Acknowledgements

K.P.R. acknowledges funding from the National Research Council Research Associateship Program. Some of this work was performed at the Colorado Nanofabrication Laboratory supported in part by the NNIN and the National Science Foundation under Grant No. ECS-0335765. The authors thank Dr. Dale Newbury and Dr. Roy Geiss for helpful discussions.

References

Brodusch, N., Demers, H. & Gauvin, R. (2013a) Nanometres-resolution Kikuchi patterns from materials science specimens with transmission electron forward scatter diffraction in the scanning electron microscope. *J. Microsc.* **250**, 1–14.

Brodusch, N., Demers, H., Trudeau, M. & Gauvin, R. (2013b) Acquisition parameters optimization of a transmission electron forward scatter diffraction system in a cold-field emission scanning electron microscope for nanomaterials characterization. *Scanning*, **35**, 375–386.

Chen, G.H., Hou, Z.F. & Gong, X.G. (2008) Structural and electronic properties of cubic HfO(2) surfaces. *Comput. Mater. Sci.* **44**, 46–52.

Deal, A., Hooghan, T. & Eades, A. (2008) Energy-filtered electron backscatter diffraction. *Ultramicroscopy* **108**, 116–125.

Dingley, D. (2004) Progressive steps in the development of electron backscatter diffraction and orientation imaging microscopy. *J. Microsc.* **213**, 214–224.

Geiss, R., Keller, R. & Read, D. (2010) Transmission electron diffraction from nanoparticles, nanowires and thin films in an SEM with conventional EBSD equipment. *Microsc. Microanal.* **16**, 1742–1743.

Hu, J. & Pan, B.C. (2009) Surface effect on the size- and orientation-dependent elastic properties of single-crystal ZnO nanostructures. *J. Appl. Phys.* **105**, 034302–034306.

Humphreys, F.J. (1999) Quantitative metallography by electron backscattered diffraction. *J. Microsc.* **195**, 170–185.

Jagannadham, K. (2011) Orientation dependence of thermal conductivity in copper-graphene composites. *J. Appl. Phys.* **110**, 074901–074906.

Jagar, S., Wang, H. & Chun, M. (2001) Effects of longitudinal and latitudinal grain boundaries on the performance of large-grain polysilicon MOSFET. *IEEE Electr. Device Lett.* **22**, 218–220.

Joy, D.C. (1991) An introduction to Monte-Carlo simulations. *Scan. Microsc.* **5**, 329–337.

Joy, D.C. & Luo, S. (1989) An empirical stopping power relationship for low-energy electrons. *Scanning* **11**, 176–180.

Keller, R.R. & Geiss, R.H. (2012) Transmission EBSD from 10 nm domains in a scanning electron microscope. *J. Microsc.* **245**, 245–251.

Kleibert, A., Rosellen, W., Getzlaff, M. & Bansmann, J. (2011) Structure, morphology, and magnetic properties of Fe nanoparticles deposited onto single-crystalline surfaces. *Beilstein J. Nanotechnol.* **2**, 47–56.

Lanza, M., Zhang, K., Porti, M., Nafria, M., Shen, Z. Y., Liu, L. F., Kang, J. F., Gilmer, D. & Bersuker, G. (2012) Grain boundaries as preferential sites for resistive switching in the HfO[sub 2] resistive random access memory structures. *Appl. Phys. Lett.* **100**, 123508–123504.

Maitland, T. & Sitzman, S. (2007) Electron backscatter diffraction (EBSD) technique and materials characterization examples. *Scanning Microscopy for Nanotechnology Techniques and Applications* (ed. by W. Zhou & Z. L. Wang), pp. 41–75. Springer, New York.

Niinistö, J., Mäntymäki, M., Kukli, K., Costelle, L., Puukilainen, E., Ritala, M. & Leskelä, M. (2010) Growth and phase stabilization of HfO_2 thin films by ALD using novel precursors. *J. Cryst. Growth* **312**, 245–249.

Prior, D.J., Boyle, A.P., Brenker, F., *et al.* (1999) The application of electron backscatter diffraction and orientation contrast imaging in the SEM to textural problems in rocks. *Am. Miner.* **84**, 1741–1759.

Roh, J.W., Hippalgaonkar, K., Ham, J.H., *et al.* (2011) Observation of anisotropy in thermal conductivity of individual single-crystalline bismuth nanowires. *ACS Nano.* **5**, 3954–3960.

Small, J.A., Michael, J.R. & Bright, D.S. (2002) Improving the quality of electron backscatter diffraction (EBSD) patterns from nanoparticles. *J. Microsc.* **206**, 170–178.

Trimby, P.W. (2012) Orientation mapping of nanostructured materials using transmission Kikuchi diffraction in the scanning electron microscope. *Ultramicroscopy* **120**, 16–24.

Vanasupa, L., Joo, Y.C., Besser, P.R. & Pramanick, S. (1999) Texture analysis of damascene-fabricated Cu lines by x-ray diffraction and electron backscatter diffraction and its impact on electromigration performance. *J. Appl. Phys.* **85**, 2583–2590.

Vinci, R.P. & Vlassak, J.J. (1996) Mechanical behavior of thin films. *Annu. Rev. Mater. Sci.* **26**, 431–462.